DOI: 10.13009/EUCASS2022-7664
9TH EUROPEAN CONFERENCE FOR AERONAUTICS AND SPACE SCIENCES (EUCASS)

Design, modelling and prototyping of a single-material composite tank for cryogenic propellant storage

Tanguy Briand[1], Jerome Benabes[1], Antoine Lavaud[1], Yann Accettura[1], Yann Farenc[1], Elena Carcano[1], Vanessa Gaubert[1], Sébastien Paul[1], Laurent Lagunegrand[1], Sylvain Pernon[2], Yannick Guerin[2], Jean-Pierre Mazel[2]

[1]*CMP Composites, 17 Impasse du Taillan, 33320 EYSINES*
[2]*CNES, 2 Place Maurice Quentin, 75001 PARIS*

Abstract

PERSEUS project allows a quick development and testing of innovative technologies to optimize the performance of today's launchers. In this context, CMP Composites and CNES have developed an innovative design for a cryogenic tank made entirely of composite material from the liner to the base, including the structural part and the skirt, allowing a significant gain in production and launch costs (thanks to the reduction of the tank mass). The modelling and validation tests carried out so far allow to validate the chosen strategy. In this article we describe the entire methodology for the design and manufacture of the tank which is now being successfully tested under cryogenic conditions (-196 °C) and up to 60 bar internal pressure.

1 Introduction

The development of the space industry relies on a significant reduction in the manufacturing and launch costs of launchers. One of the main lines of research linked to this problem lies in the manufacture of linerless composite tanks for the storage of liquid propellants [Reed, 2016, Liu et al., 2021].

Liquid propellant tanks can contain cryogenic fluids ranging from 110 K to 20 K (LN2, LHe, LCH4). These very low temperatures coupled with the internal pressurization and the general forces applied to the tank during launch induce a significant thermomechanical loading on the structure. Due to the differential expansion between the anisotropic layers of the composite, the mere cooling of the tank generates an initial stress state in the material depending on the lamination [Schutz, 1998, Aoki et al., 2001, Kumazawa and Whitcomb, 2008, Wei et al., 2015]. A thermomechanical load, even one that is small in relation to the failure limit, can initiate and propagate damage within the material. This damage results in microscopic mechanisms (fibre-matrix decohesion, micro-cracking, fibre breakage) and mesoscopic mechanisms (transverse cracking, delamination at the crack tip, fibre strand failure). Depending on the architecture of the material and the applied load, a damage scenario is established. During this scenario, the stress state in each ply and the interaction phenomena between the plies induce the initiation and propagation of intra- and inter-laminar cracking. The coalescence of the damage then generates a network of cracks [Lavoie and Adolfsson, 2001, Yokozeki et al., 2005, Kim et al., 2006, Kim and Donaldson, 2006, Kumazawa et al., 2006].

This phenomenology leads to the introduction of a leak criterion in addition to the failure criterion for the design of a linerless tank. Moreover, this criterion can be very penalising and lead to a very high mass compared to a solution meeting only the failure criterion. Thus, a detailed analysis of the mechanisms leading to the loss of tightness is essential to propose an industrially viable design.

DOI: 10.13009/EUCASS2022-7664

The elasto-damageable behaviour of the composite is governed by the mechanical properties of the material's constituents (stiffness and strength of the matrix, fibres and interfaces) but also by numerous geometric parameters (thickness, position and orientation of the layers, arrangement of the fibres). The design becomes more complex in presence of specific cryogenic fluids (LOX) because the compatibility between the fluid and the tank materials strongly limits the choice of the structure's components [Malenfant, 2012].

In this sense, within the framework of the PERSEUS project and the development of the ASTREOS launcher, CMP Composites in collaboration with CNES is developing a full-composite tank (base, liner, structure, skirt) based on an innovative design involving several composite manufacturing processes (infusion and filament winding).

This article provides an overview of the development of the composite cryogenic tank. First, we will present the design principles, the materials and the implementation processes used to manufacture the tank. Afterwards, we will present the sizing strategy based on a purely numerical approach with a modelling of the non-damageable elastic behaviour of the composite at the mesoscopic scale. This sizing step allows to validate the global criteria of the structure (strength and stiffness) and to evaluate the criticality of the different links [Mason et al., 2015]. The different stages of validation of these connections will then be presented. Finally, the qualification tests of the tank will be presented as well as a vision of the evolution of the tank during these tests. We will end with a discussion of the results obtained on these first tanks in order to conclude on the innovative technologies and concepts developed by CNES and CMP Composites. In addition, the prospects for this work, which is still evolving and being optimised, will be described.

2 Design, materials and manufacture process

One of the major difficulties in the development of cryogenic tanks is the management of differential expansion. In order to minimise these effects, CMP Composite proposes to produce a composite liner infused in a single operation with a composite block which will serve as a connection base after polymerisation and machining. This base/liner part will also be used as a winding mandrel for the tank and skirt parts.

The liners and bases are made by vacuum infusion. They are draped with dry carbon fibre fabric over a pre-treated aluminium mandrel. A specific draping strategy was developed to obtain a circular part that is as homogeneous as possible. Depending on the areas being draped (base or liner), we choose to use wovens with different surface mass in order to optimise the thickness and ease of draping. The considerable thickness of the base section required fine-tuning of the infusion parameters. Macro and microscopic sections allowed to validate the correct impregnation of the material.

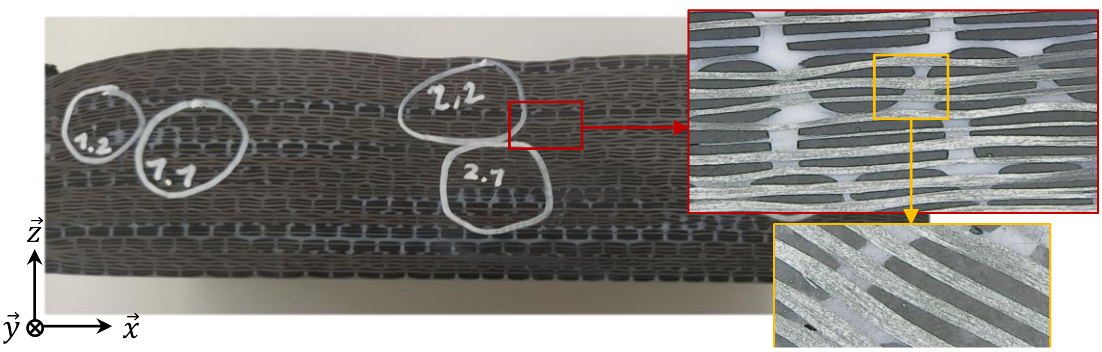

FIGURE 1 – Macro and microscopic sections of an infusion test on a thick specimen.

DOI: 10.13009/EUCASS2022-7664

The "one-shot" infusion of half-liners/bases, assembled later, allows the integration of particular systems (anti-vortex, anti-sloshing, diffuser) inside the tank during the manufacturing process. At this stage of the manufacturing process, it is also possible to apply an internal coating to the tank in order to improve its tightness and/or the compatibility of the structure with the stored fluid (LOX) [Malenfant, 2012].

The liner/base assembly manufactured this way, is now used as a winding mandrel for the structural part of the tank using a dedicated tooling. The tank is manufactured with a wet winding process using high-strength dry fibres and an epoxy resin [Pilato, 2011]. The stacking sequence of the structural part is identified during the design phases presented in paragraph 3. The winding process requires the definition of several parameters such as the width and thickness of the deposited strip (composed of several wicks) as well as the winding angle. From these parameters and Clairaut's relations, we can define a geodesic trajectory on which the fibre will land in a stable manner. The mandrel is covered by the repetition of this trajectory for a number of cycles obtained from the perimeter of the mandrel and the width of the band along the circumferential direction. This way, we manufacture a layer with plies oriented at $\pm$ the angle of deposition and of thickness equal to two that of the deposited wick. Depending on the geometry of the mandrel and the impregnation rate, the strip width can vary during the winding of ± 10 % and thus induce overlaps or gaps between the deposited strips [Lan, 2016]. In the case of V-type tanks, it seems preferable to avoid the gaps in which the cracking can propagate [Briand et al., 2019]. As a result, we will favour a slight overlap in our filament winding manufacturing strategy which allows us to minimise resin rich areas in the wound part. The programming of the filament winding was carried out on dedicated software. Longitudinal layers are mainly used to take up the axial forces of the tank and are tangential to the base neck. Circumferential layers (figure 2a) take up the radial forces of the tank. Finally, layers at intermediate angles complete the stratification. These layers increase the tank's shear strength and can carry some of the stresses in the two main directions.

Once the tank has been wound and before polymerisation, a tool is used to wind the skirt. This process (co-curing) allows for a chemical bonding of the resin between the skirt and the tank, which is much more interesting from a thermo-mechanical point of view than joining the two cured parts by gluing. Therefore, at the end of the tank winding, we put in place the skirt winding tooling, previously treated with a release agent. The skirt is then wound following a stacking sequence identified in the design phase in order to carry the structural forces acting on the launcher.

Once the resin curing cycle has been completed, the tooling is removed and the tank's skirts are cut to length (figure 2b).

NDA techniques were applied to evaluate the health of the tank. An inspection was carried out by ultrasound and by X-ray tomography (Flat-Panel Volume Computed Tomography). The X-ray measurements were carried out with a resolution of about 160 µm. We can make some minor remarks on the general condition of the tank. It can be noted that winding the tank and skirt together before the resin had set allowed the creation of a bead of resin at the interface between tank and skirt. This can help to lower the stress concentrations in this area [Mason et al., 2015]. Overall, at the resolution level of this test, we do not observe any macroscopic defects ($>$160 µm) in the reservoir and at the various bonds. Post-reservoir qualification observations using high resolution NDT or microscopy will allow us to refine these initial analyses.

DOI: 10.13009/EUCASS2022-7664

(a) Circumferential layer.

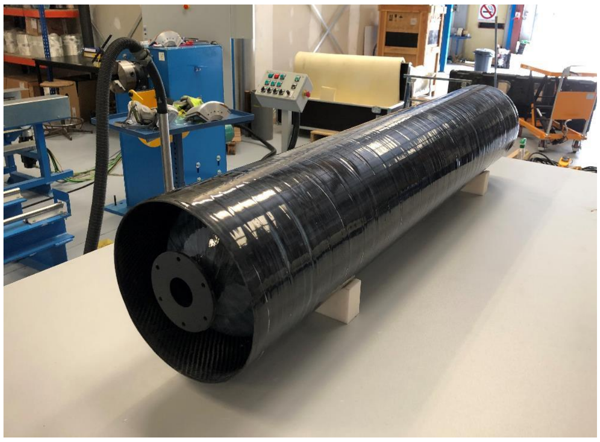

(b) Global view

FIGURE 2 – Manufacture of the tank and skirts

3 Tank sizing

3.1 Modeling strategy and sizing criteria

The design of the tank goes through several steps which aim at studying the global behaviour of the tank and its connections using models and experimental tests of increasing complexity.

In the first stage, our strategy aims to numerically sizing the tank so that it meets macroscopically the criteria of composite sizing. The tank is designed under thermo-mechanical loading, internal pressure of 60 bars at -182 °C (LOX boiling temperature). Both criteria are defined as below :

1. Strength criterion : The allowable stress in the fibre direction must not be exceeded ;
2. Tightness criterion : The permissible strain in the transverse direction of the fibre must not be exceeded.

The second criterion is generally very conservative with respect to the strength criterion because the transverse behaviour of the fibre is governed by the matrix of the composite. However, in the context of a V-type tank design, it is essential to take this criterion into account if the tank is to be kept leak-free. Indeed, as mentioned in the introduction, exceeding the transverse strain criterion in the ply onsets the appearance of matrix cracks which, through interaction with the plies, tend to propagate rapidly through the thickness of the laminate, leading to an abrupt decrease in the tightness of the structure [Laeuffer, 2017]. Thus, we will rely on this second criterion to identify the stratification of our tank. This criterion was identified from transverse cracking tests on cross-laminated specimens under load, during which we can quantify the transverse cracking kinetics of our fibre/matrix couple [Huchette, 2005].

The other critical interfaces of the tank will be designed using the failure criteria where we will try not to exceed the ultimate strength in the three directions of the orthotropy plane of the plies of our laminates.

The criticality of the different elements is evaluated through this first macroscopic model. This analysis then allows us to set up more precise models to evaluate the behaviour of certain zones in greater detail. These areas of high criticality, such as the base/liner or tank/skirt connection, will also be the subject of a test/calculation dialogue to ensure a more accurate design.

DOI: 10.13009/EUCASS2022-7664

3.2 Global model 3D

3.2.1 Description

The global model is presented in figure 3. In this model, the composite part is modelled with 3D shell elements while the rest of the parts are modeled as 3D solids. A rigid link is applied at the connection between the screws and the composite base. Generalized contact conditions are implemented between all other surfaces that are or will be in contact. We apply an internal pressure of 60 bars.

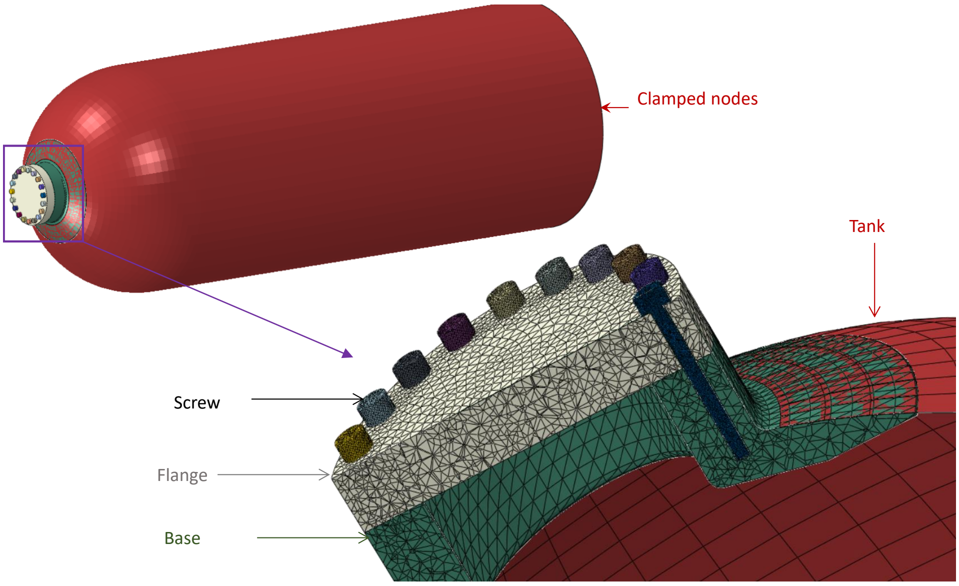

FIGURE 3 – Presentation of the first validation model of the solution

3.2.2 Results

First, we iterate on the angles of the lamination to determine a configuration in which we do not exceed both the strength and tightness criteria. The tank structure was modelled in Abaqus using the dedicated filament winding plug-in, which allows us to carry our calculation of stress and strain in each of the plies and angular sectors of the tank (bottom and shell). Once the criteria described above have been validated, we move on to the study of the different parts of the tank.

We check the strength of the metal parts (flange and screws) using the equivalent Von Mises criterion in stress. The elastic limit is not reached on the current part of the screw. A stress concentration is observed below the screw heads (465 MPa), which remains below the permissible strength of the screws (A4-70 stainless steel, Re=700 MPa) and which will be mitigated by the introduction of a washer.

On the base side, we look at the out-of-plane stress in order to avoid failure at the inter-laminar interface (figure 4). The out-of-plane allowable is initially set at 50 MPa. As we assumed following a failure during a first stamping, this admissible seems to be lowered by the constraints linked to the process (interface thickness, heterogeneity, stress concentration). This first test tends to attenuate the out-of-plane allowable by about 50 % and indicates an important criticality of the bond. However, the model proposed in this first study does not correctly represent the end-cap geometry generated by the closure of the longitudinal plies on the baseplate during winding. The shell model underestimates the material quantity in the area. This particular geometry, decribed by a local over-thickness, is representative of a filament winding process. It allows the baseplate to be confined and minimises the stress concentration in the fillet.

DOI: 10.13009/EUCASS2022-7664

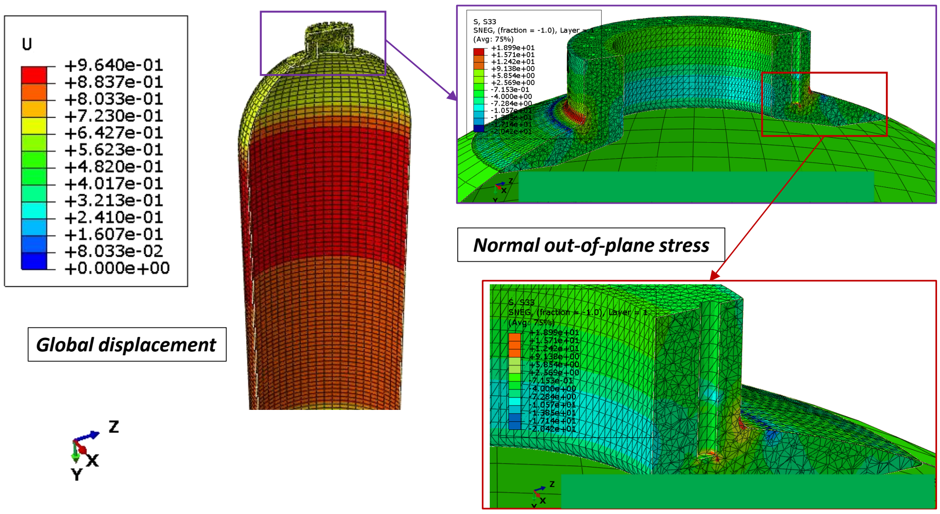

FIGURE 4 – Out-of-plane stress analysis in the composite base

3.3 Axi-symetric cohesive model

3.3.1 Description

In order to study this particular zone between the base and the over-thicnkess of the tank part made in filament winding, it would be necessary to model the tank in 3D volume elements. However, as we have already validated the resistance of the screws during the experimental test and the first numerical model presented before, we propose an axi-symmetrical modelling of the assembly (figure 5) in which we will be able to mesh very finely in order to study the connection between the base and the tank. Not knowing how this connection behaves (completely unglued or completely glued), we introduce a cohesive zone between the two surfaces. This cohesive zone allows us to observe a degradation of the bond if it should occur.

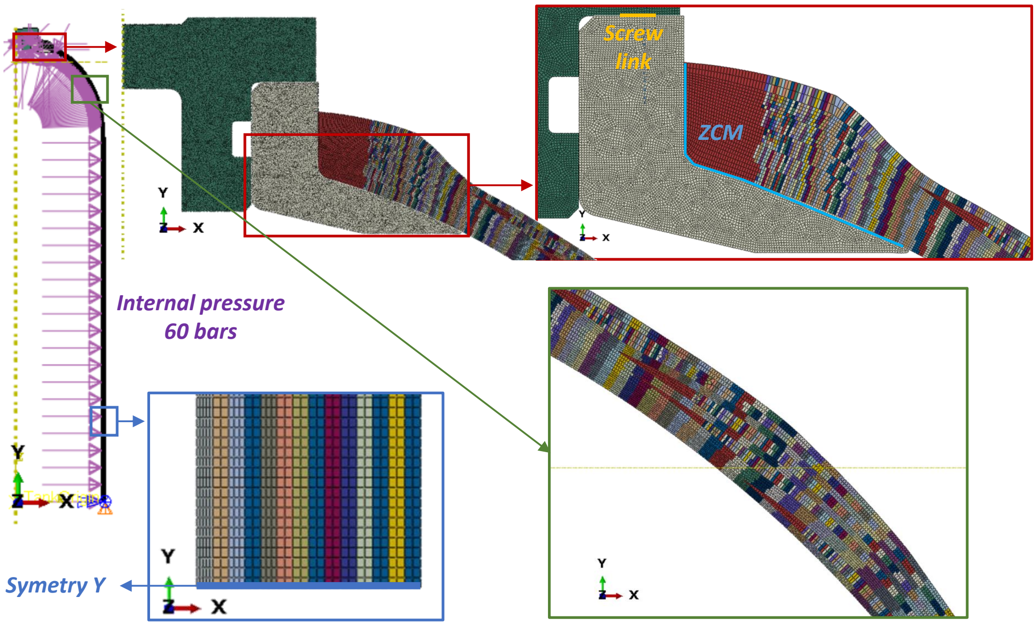

FIGURE 5 – Presentation of the axi-symetric model

DOI: 10.13009/EUCASS2022-7664

We implement cohesive properties, summarised in Table 1, from the literature on inter-laminar cracking modelling [Camanho et al., 2003, Turon et al., 2007, Iarve et al., 2011, Grogan et al., 2015]. The cohesive zone models a bi-linear behaviour of the interface based on a quadratic stress criterion and an energetic damage evolution governed by the Benzeggagh-Kenane criterion [Benzeggagh and Kenane, 1996]. A rigid connection is modelled on the diameter of the screw between the base and the stamping flange. Generalized contact conditions are introduced between the rest of the surfaces. A symmetry condition along the Y axis is introduced to fully constrain the model and an internal pressure of 60 bars is applied (tank test pressure).

Set	Kn	Ks	Kt	σ_n	σ_s	σ_t	G_n	G_s	G_t	η	τ
		$N.mm^{-3}$			MPa			$mJ.mm^{-2}$		-	sec.
Initial	10^6	10^6	10^6	50	80	80	100	500	500	1	0.0001

TABLE 1 – Cohesive model : Litterature set parameters

3.3.2 Results

The model results do not show significant damage to the cohesive zone even when halving the literature data. There is only an initiation of damage at the edges of the interface which seems logical. However, the damage does not propagate along the interface. In fact, we assume that the loading should not cause the interface between the base and the tank to lift off. Thus, the normal out-of-plane stress in the composite baseplate does not exceed the allowable ($\sigma_{33} < 5$ MPa) even when knocked down by the process stresses.

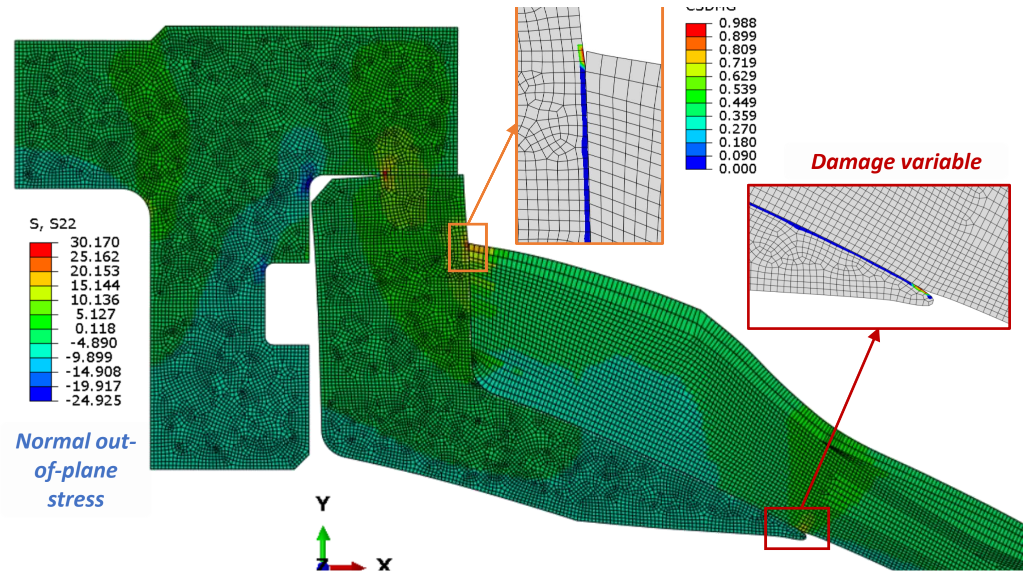

FIGURE 6 – Response of the axi-symmetric model for the study of the base/reservoir interface

In conclusion, we believe that the solution is appropriate to continue the qualification of the tank. However, we remain vigilant about the strength of the tank/plane interface. Indeed, the proposed modelling seems to indicate that the interface will hold. On the other hand, this type of damage phenomenon is very difficult to model and to capture numerically because of its complexity. For example, if the interface were to crack completely, the fillet could become over-stressed and, according to the modelling we have carried out in this most critical case, the base would fail at the fillet (out-of-plane stress = 35 MPa > Stress at failure of the semi-structural test but lower than the admissible one initially used). This would result in ejection of the upper part of the base plate and the metal sealing flange. Therefore, we will take the necessary precautions to avoid material and physical damage should this critical case occur.

DOI: 10.13009/EUCASS2022-7664

3.4 Validation of the base connection

3.4.1 Validation strategy

Our strategy for validating our critical connections is to set up one or more experimental tests to establish design criteria in dialogue with numerical models. We present here the protocol for the design of our connection between the base, the liner and the sealing flange. On one of our V-type tank models, we identified the connection screwed directly into the composite as an interesting solution. It is this design that is presented here.

When the tank is pressurised internally, the pressure is applied to the sealing flange, which transmits the forces back into the base through our screw connection. In fact, the threads are mainly loaded in mode I of pull-out. In order to study the influence of the length and diameter of the thread to be used, we first set up a pull-out test on an elementary specimen. This test allowed us to identify the optimum configuration for our baseplate. A semi-structural test on a single base will then be carried out to validate our configuration before launching the manufacture of the tank.

3.4.2 Identification of an optimal configuration

In order to evaluate the pull-out strength of a composite thread as a function of the implantation length and the diameter of the screw, we set up a test set-up presented in figure 7. It consists of pulling under the head of a screw implanted in a composite block that we will designate as an elementary test piece representative of the microstructure of the composite base of our final tank. A flange connected to the frame of the 150 kN tensile machine allows us to keep the elementary specimen fixed during the screw tensile test. A model of the test (figure 7) allowed us to validate the strength of the assembly and the stress field generated in the specimen. We have also validated that the bending in the tensile zone and therefore the shear mode of stress will be negligible compared to the pull-out mode.

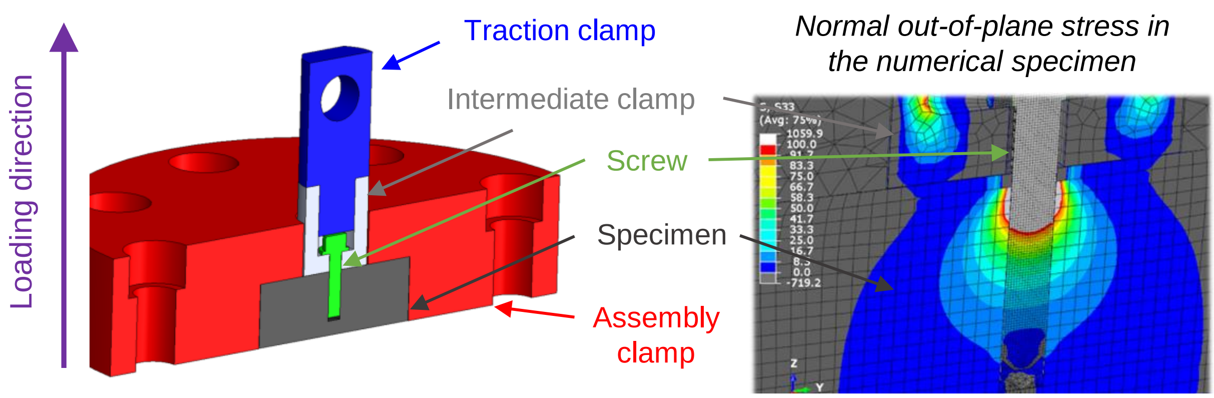

FIGURE 7 – Presentation of the concept of the pull-out test on elementary specimens

DOI: 10.13009/EUCASS2022-7664

The test campaign allowed us to evaluate a number of pull-out configurations but also to qualify the pull-out behaviour of a screwed connection. The figure 8 shows the pull-out behaviour of a screwed connection in a composite paving stone. We notice that the behaviour is not monotonic and that it can be distinguished in three phases :

1. A first phase, called **accommodation**, during which the behaviour is non-linear and increases with an increase in the stiffness of the bond. It is assumed that each of the threads of the connection is put under tension, particularly the deepest threads which are initially less loaded than those at the edges of the holes. The connection then gains in stiffness and tends towards a constant and nominal stiffness for the current configuration ;
2. A second phase, called **evolution**, during which all the threads work together following a load distribution established according to the depth of the thread. The behaviour of the connection is nominal with a constant stiffness representative of it ;
3. A third and final phase, known as the **degradation** phase, in which the behaviour of the link is non-linear and decreasing with a loss of link stiffness. We assume that the threads degrade progressively from the most loaded threads (edge of the hole) to the least loaded threads (bottom of the thread) until the link fails completely. The load transfer between the threads becomes more and more violent, which leads to an increase in non-linearity during the degradation process.

In our approach of pre-design and not of optimization, we will choose to place ourselves in the first phase of accommodation which allows us to secure the bond with regard to dispersions and possible cycling. A configuration of the link is therefore established from these tests governed by the diameter of the screws, their implantation length and the number of screws in the link.

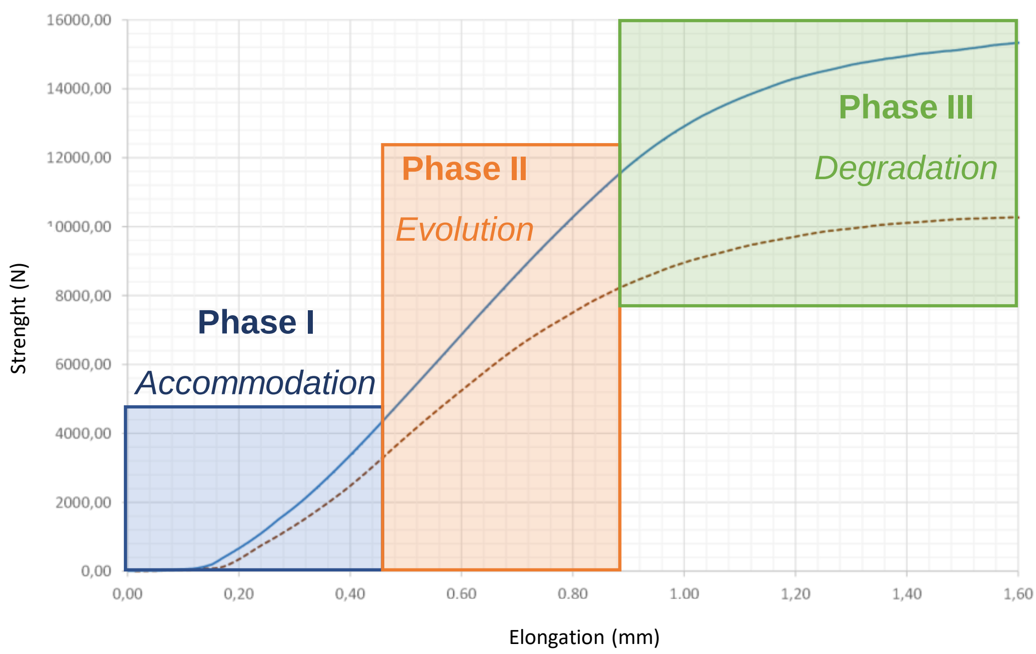

FIGURE 8 – Results and phenomenology of the pull-out test on elementary specimens

DOI: 10.13009/EUCASS2022-7664

3.4.3 Validation on semi-structure

In order to confirm the configuration chosen from the elementary tests, we propose to carry out a semi-structural test on a composite baseplate alone. The figure 9 presents the concept of the test setup. The idea is to stress a composite baseplate out of plane by pulling on a flange that is threaded into the baseplate. The baseplate is held on a fixed frame with a flange that has the curved shape of the baseplate in order to reproduce reality as closely as possible. The pull on the upper flange will then model the internal pressure of the tank. We will therefore try to verify that the force at rupture is greater than the resultant from the internal pressure.

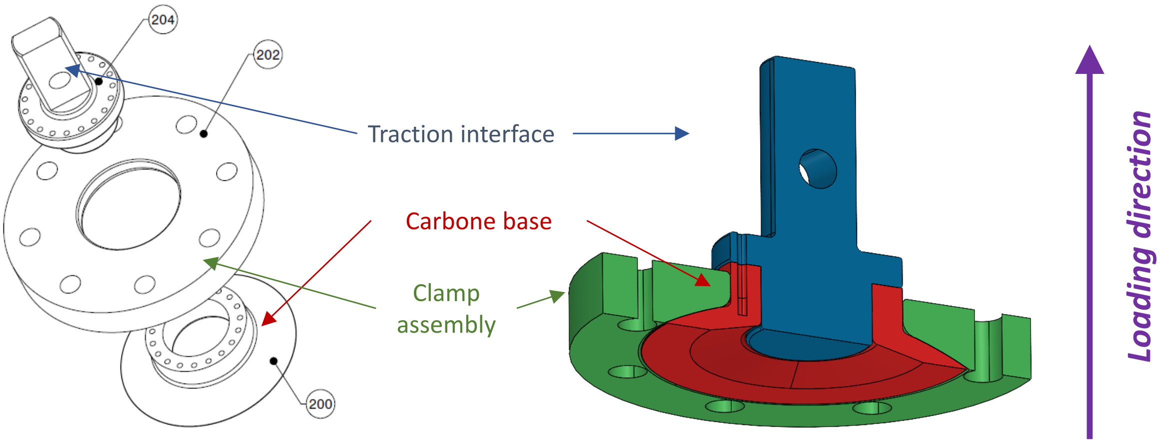

FIGURE 9 – Presentation of the concept of the semi-structural pull-out test on the carbon base

A numerical validation was carried out on the proposed concept figure 9. The 3D volume model can be seen in figure 10. The test set-up has two planes of symmetry which we have exploited to minimise the calculation time. Then, the part of the lower flange in contact with the frame is recessed since it is assumed that the 8 M16 screws are sufficient to properly clamp the flange and that this area is infinitely rigid compared to the rest of the assembly. A reference node is coupled to the upper surface of the tension flange. We apply a force equivalent to the force obtained in the test presented below, i.e. 11.5 kN, knowing that the target force to take up the pressure force is 7.5 kN (60 bars on a 40 mm diameter surface). The screws are linked to the baseplate by threads which we model as a rigid link between the nodes of the facing surfaces. General contact conditions are introduced for the rest of the surfaces that are expected to meet during the test.

The results of the numerical modelling figure 10 show a stress concentration in the fillet at the foot of the base barrel. The curve shows a stress level close to 24 MPa at the fillet level but which decreases very significantly as one moves towards the inside of the base. Indeed, 1 mm further inwards, the out-of-plane stress level drops to 12.5 MPa. Given the initial allowable stress (50 MPa), the baseplate should not fail at this loading level. On the other hand, the conclusions of the experimental test in the next section will show that our analyses of the first failure on the tank stamping seem to be relevant and that the first admissible used is shot down by the geometry and the heterogeneities generated by the manufacturing process. Overall, the numerical simulation indicates that the assembly holds up before the specimen breaks and prompts us to launch the test presented next.

DOI: 10.13009/EUCASS2022-7664

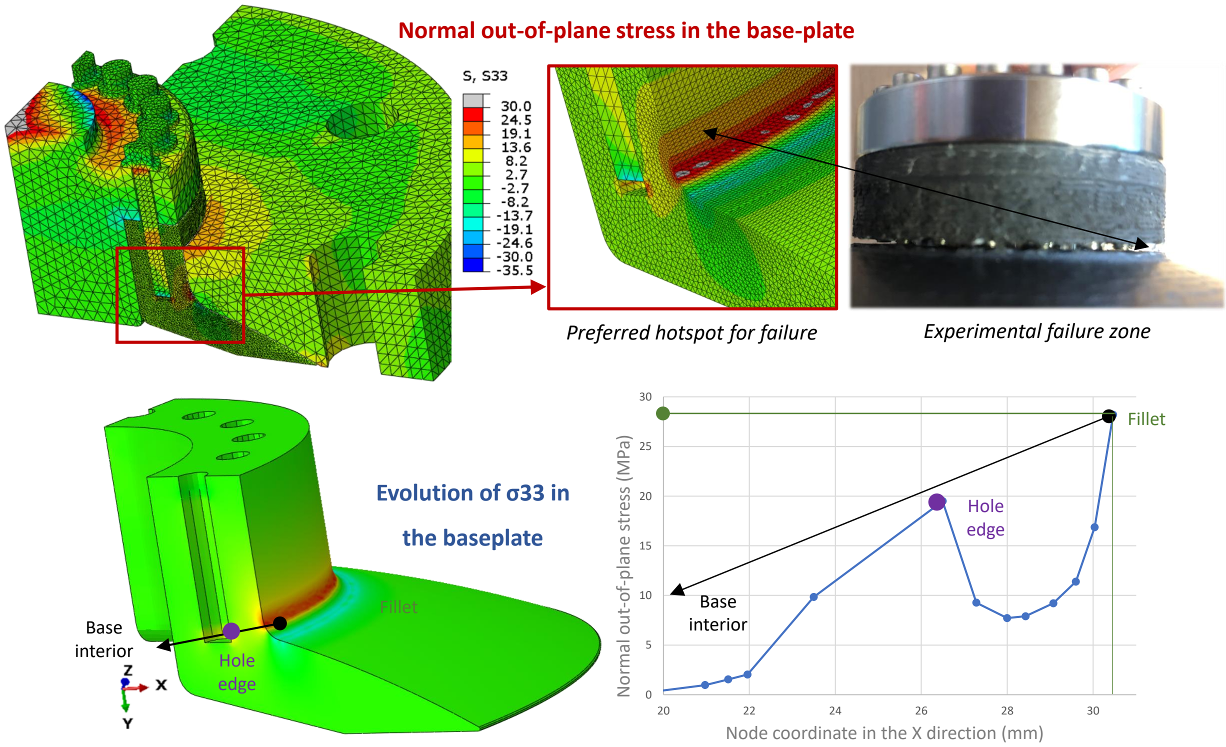

FIGURE 10 – Results of the numerical simulation of the pull-out test

Once the numerical validation had been completed and the strength of the fixture validated for the targeted failure force, the machining of the test tooling was initiated. A composite base was machined from an infused plate. The other two parts are standard steel. The CHC screws are A4-70 stainless steel with a yield strength of 700 MPa. The assembly is flanged to a 150 000 kN capacity tensile machine using the frame flange and the eight M16 screws shown in figure 9. The tensile flange is connected to the tensile clevis with a fitted pin. The test is controlled with an imposed force of 1500 N/min, which corresponds to pressurising the tank to 60 bar in 30 min. The objective of the test is to achieve an axial force equivalent to a pressure of 60 bar applied to a circular section of 40 mm diameter, i.e. 7.5 kN.

From a structural point of view, we achieved the objective initially set at 7.5 kN. The failure at 11.5 kN translates into a pressure of about 91 bars on a circular surface of diameter 40 mm. To correlate with the experimental test, we can note an average, unweighted, of the stresses recorded in figure 11 of about 9.5 MPa. Experimentally, we note a stress at rupture (force at rupture related to the rupture section) close to 8.5 MPa.

The figure 11 shows the resultant curve of one of the tensile tests we carried out on one of the configurations tested during the study. A failure of the baseplate is observed, which occurs at about 11.5 kN. The failure is clear and reflects a brittle behaviour of the connection in this direction. From a phenomenological point of view, it is interesting to note that we find the observations made on the elementary tests with the three life phases of a screwed connection in a laminated composite.

These analyses allow us to confirm our modelling choices. Also, this test-calculation dialogue allows us to validate our strategy for sizing the base connection of our tank.

DOI: 10.13009/EUCASS2022-7664

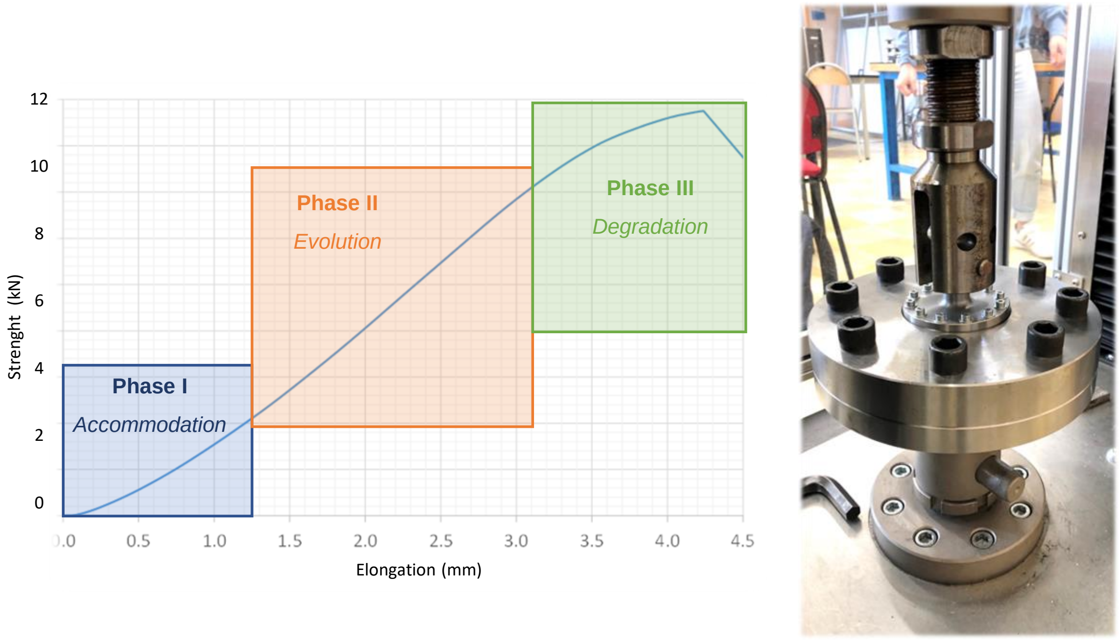

FIGURE 11 – Out-of-plane pull-out test result on the composite baseplate

4 Conclusions and perspectives

This article provides a macroscopic description of the work carried out by CMP Composites and CNES in the framework of the PERSEUS project on the manufacture of composite cryogenic tanks.

In the first part, we describe the materials and processes used to manufacture the tank. We described the innovative design of a V-shaped tank wound on a composite mandrel serving as both liner and winding core. This composite liner/mandrel is made up of two parts which are then joined together to allow the introduction of coatings or special equipment into the tank during its manufacture. Its "one-shot" infusion with a "net-shape" composite base makes it an innovative and technologically complex process to implement.

The second part presents the global design strategy of the tank based on strength and stiffness criteria according to the parts of the tank considered. First macroscopic models allow to identify the critical connections. More detailed models associated with specific experimental tests allow the validation of certain parts of the tank.

Some of the qualification tests have now been completed and a new version of the tank is in the final qualification phase. From the various tank developments, we have been able to identify numerous scientific and technological obstacles, most of which have now been overcome. The tank developed today is entirely made of composite material and has been validated under thermal loading alone (-196 °C) and under mechanical loading up to 60 bar. Qualification under thermo-mechanical loading is in progress.

The focus today is on the optimisation of the tank in order to save mass at launch and manufacturing cost. This involves a lot of work on the resin system used in order to refine our design criteria. We are also working on the impact of adding a barrier layer to our tank in order to optimise its tightness [Accettura et al., 2022]. This layer would also allow us to improve the compatibility of our tank with particular fluids such as liquid oxygen. In this sense, liquid oxygen compatible resin systems are also being studied in order to validate that these systems also validate the different dimensioning criteria of a V-type tank.

Finally, we are also working on the expansion of this type of tank design to other applications such as the storage of liquid hydrogen at low temperature and pressure, but also to the storage of gas under high pressure. This involves adapting certain parts of the current tank, such as the design and sizing of the composite base.

DOI: 10.13009/EUCASS2022-7664

Références

[Accettura et al., 2022] Accettura, Y., Briand, T., Bois, C., and Wahl, J.-C. (2022). Characterization of damage of laminated composite with a barrier layer under thermomechanical loading. *ECCM20.*

[Aoki et al., 2001] Aoki, T., Ishikawa, T., Kumazawa, H., and Morino, Y. (2001). Cryogenic mechanical properties of CF/polymer composites for tanks of reusable rockets. *Advanced Composite Materials : The Official Journal of the Japan Society of Composite Materials*, 10(4) :349–356.

[Benzeggagh and Kenane, 1996] Benzeggagh, M. L. and Kenane, M. (1996). Measurement of mixed-mode delamination fracture toughness of unidirectional glass/epoxy composites with mixed-mode bending apparatus. *Composites Science and Technology*, 56(4) :439–449.

[Briand et al., 2019] Briand, T., Bois, C., Wahl, J.-C., Le Goff, E., and Lavelle, F. (2019). Caractérisation et modélisation de la cinétique de fissuration transverse dans un composite stratifié - Effet de l'épaisseur des plis et de la température. Brest.

[Camanho et al., 2003] Camanho, P. P., Davila, C. G., and de Moura, M. F. (2003). Numerical Simulation of Mixed-Mode Progressive Delamination in Composite Materials. *Journal of Composite Materials*, 37(16) :1415–1438.

[Grogan et al., 2015] Grogan, D. M., Ó Brádaigh, C. M., and Leen, S. B. (2015). A combined XFEM and cohesive zone model for composite laminate microcracking and permeability. *Composite Structures*, 120 :246–261.

[Huchette, 2005] Huchette, C. (2005). *Sur la complémentarité des approches expérimentales et numériques pour la modélisation des mécanismes d'endommagement des composites stratifiés.* Thèse de doctorat, Université Paris 6.

[Iarve et al., 2011] Iarve, E. V., Gurvich, M. R., Mollenhauer, D. H., Rose, C. A., and Dávila, C. G. (2011). Mesh-independent matrix cracking and delamination modeling in laminated composites. *International Journal for Numerical Methods in Engineering*, 88(8) :749–773.

[Kim and Donaldson, 2006] Kim, R. and Donaldson, S. (2006). Experimental and analytical studies on the damage initiation in composite laminates at cryogenic temperatures. *Composite Structures*, 76(1-2) :62–66.

[Kim et al., 2006] Kim, R., Sihn, S., and Donaldson, S. (2006). Effect of ply thickness on the damage development in composite laminates. volume 51.

[Kumazawa et al., 2006] Kumazawa, H., Aoki, T., and Susuki, I. (2006). Influence of stacking sequence on leakage characteristics through CFRP composite laminates. *Composites Science and Technology*, 66(13) :2107–2115.

[Kumazawa and Whitcomb, 2008] Kumazawa, H. and Whitcomb, J. (2008). Numerical Modeling of Gas Leakage Through Damaged Composite Laminates :. *Journal of Composite Materials.*

[Laeuffer, 2017] Laeuffer, H. (2017). *Caractérisation et prédiction du réseau de fissures dans les composites stratifiés - Application aux réservoirs de lanceurs spatiaux sans liner.* Thèse de doctorat, ENSAM ParisTech.

[Lan, 2016] Lan, M. (2016). *Étude de l'influence des singularités créées par la technique de placement de fibres automatisé sur les performances des matériaux composites.* Thèse de doctorat, Université de Bretagne Sud.

[Lavoie and Adolfsson, 2001] Lavoie, J. A. and Adolfsson, E. (2001). Stitch Cracks in Constraint Plies Adjacent to a Cracked Ply. *Journal of Composite Materials*, 35(23) :2077–2097.

DOI: 10.13009/EUCASS2022-7664

[Liu et al., 2021] Liu, N., Ma, B., Liu, F., Huang, W., Xu, B., Qu, L., and Yang, Y. (2021). Progress in research on composite cryogenic propellant tank for large aerospace vehicles. *Composites Part A : Applied Science and Manufacturing*, 143 :106297.

[Malenfant, 2012] Malenfant, J.-C. (2012). *Étude de l'influence de l'endommagement sur la perméabilité des matériaux composites, application à la réalisation d'un réservoir cryogénique sans liner*. Thèse de doctorat, Université Bordeaux 1.

[Mason et al., 2015] Mason, B. H., Sleight, D. W., and Grenoble, R. (2015). Test and Analysis Correlation for a Y-Joint Specimen for a Composite Cryotank.

[Pilato, 2011] Pilato, A. (2011). *Caractérisation des structures composites bobinées épaisses, application à l'étude du comportement de réservoirs de stockage d'hydrogène*. Thèse de doctorat, Université Bordeaux I.

[Reed, 2016] Reed, J. G. R. (2016). Performance Efficient Launch Vehicle Recovery and Reuse. Long Beach, CA, United States.

[Schutz, 1998] Schutz, J. B. (1998). Properties of composite materials for cryogenic applications. *Cryogenics*, 38(1) :3–12.

[Turon et al., 2007] Turon, A., Dávila, C. G., Camanho, P. P., and Costa, J. (2007). An engineering solution for mesh size effects in the simulation of delamination using cohesive zone models. *Engineering Fracture Mechanics*, 74(10) :1665–1682.

[Wei et al., 2015] Wei, W., Rongjin, H., Chuanjun, H., Zhao, Y., Li, S., and Laifeng, L. (2015). Cryogenic performances of T700 and T800 carbon fibre- epoxy laminates. *IOP Conference Series : Materials Science and Engineering*, 102 :012016.

[Yokozeki et al., 2005] Yokozeki, T., Aoki, T., Ogasawara, T., and Ishikawa, T. (2005). Effects of layup angle and ply thickness on matrix crack interaction in contiguous plies of composite laminates. *Composites Part A : Applied Science and Manufacturing*, 36(9) :1229–1235.